

SUZAKU OBSERVATIONS OF THE GALACTIC CENTER MICROQUASAR 1E 1740.7-2942

MARK T. REYNOLDS¹, JON M. MILLER¹*Draft version May 10, 2010*

ABSTRACT

We present two *Suzaku* observations of the Galactic center microquasar 1E 1740.7-2942 separated by approximately 700 days. The source was observed on both occasions after a transition to the spectrally hard state. Significant emission from 1E 1740.7-2942 is detected out to an energy of 300 keV, with no spectral break or turnover evident in the data. We tentatively measure a lower limit to the cut-off energy of ~ 380 keV. The spectra are found to be consistent with a Comptonized corona on both occasions, where the high energy emission is consistent with a hard power-law ($\Gamma \sim 1.8$) with a significant contribution from an accretion disc with a temperature of ~ 0.4 keV at soft X-ray energies.

The measured value for the inner radius of the accretion disc is found to be inconsistent with the picture whereby the disc is truncated at large radii in the low-hard state and instead favours a radius close to the ISCO ($R_{\text{in}} \sim 10 - 20 R_g$).

Subject headings: accretion, accretion disks — black hole physics — X-rays: binaries — X-rays: individual (1E 1740.7-2942)

1. INTRODUCTION

Since the discovery of apparently super-luminal jets from the X-ray binary GRS 1915+105 (Mirabel & Rodriguez 1994), the Galactic microquasars have assumed a position of critical importance in our efforts to understand accretion physics and relativistic jet production (Mirabel 1999). 1E 1740.7-2942 was discovered by the *Einstein* satellite (Hertz et al. 1984). Subsequent observations revealed 1E 1740.7-2942 to be the dominant source of hard X-rays (> 20 keV) in the direction of the Galactic center (Skinner et al. 1987, 1991), where the source is located approximately 50 arcmin from Sgr A*. The microquasar nature of 1E 1740.7-2942 was discovered upon the observation of a double sided radio jet consistent with the X-ray position (Mirabel et al. 1992). Further VLA observations showed this radio source to be highly variable (Heidl et al. 1994).

Since its discovery 1E 1740.7-2942 has been observed on numerous occasion at X-ray wavelengths. The column density towards this source is high given the proximity to the Galactic center and has been measured by *Chandra* to be $\sim 1 \times 10^{23} \text{ cm}^{-2}$ (Gallo & Fender 2002). Here, the spectrum was found to be consistent with a power-law ($\Gamma \sim 1.4$). *INTEGRAL* low-hard state observations have detected 1E 1740.7-2942 up to energies of ~ 600 keV, where the spectrum is found to be consistent with a power-law ($\Gamma \sim 1.6$) up to 200 keV, with an additional component required at higher energies (Bouchet et al. 2009), see also Del Santo et al. (2005) for earlier *INTEGRAL*/*RXTE* observations. In the high-soft state, the hard X-ray flux decreases significantly, dropping below the *INTEGRAL* detection limit at energies > 50 keV (Bouchet et al. 2009). Smith et al. (2002) reported on 5 years of *RXTE* monitoring, where they discovered a modulation with a period 12.73 ± 0.05 days which is attributed to the orbital period of the binary, in addition

to a possible super-orbital modulation with a period of ~ 600 days.

As the extinction at optical wavelengths is prohibitive ($A_v \sim 50$), counterpart searches are required to take place in the infrared. While a number of candidate counterparts have been identified (Marti et al. 2000; Eikenberry et al. 2001), no variability has been observed from these, rendering them unlikely to be the actual counterpart. The current upper limit for the K_s -band magnitude of the counterpart is ≥ 19.9 at the 95% confidence level. This is equivalent to a secondary spectral type of O or B if on the main sequence or K if a giant, at an assumed distance of 8.5 kpc.

In this paper, we describe observations undertaken with the *Suzaku* X-ray observatory, while 1E 1740.7-2942 was in the low-hard state. In §2, we describe the observations and extraction of source spectra. We proceed to analyze the data in §3. In §4, these results are compared to observations of other microquasars in the hard state, and finally our conclusions are presented in §5.

2. OBSERVATIONS

1E 1740.7-2942 was observed on two separate occasions while in the low-hard state by *Suzaku* (Mitsuda et al. 2007) from 2006 October 09 02:20 UT until October 09 13:39 UT (obsid:501050010, PI: Koyama, epoch I) and from 2008 September 08 09:08 UT until September 09 21:33 UT (obsid:503011010, PI: Koyama, epoch II), see Fig. 1. Data were acquired over a broad spectral range (0.2 – 600 keV), with the X-ray imaging spectrometer (XIS: Koyama et al. 2007a) and the hard X-ray detector (HXD: Takahashi et al. 2007; Kokubun et al. 2007). The source was observed at the XIS nominal position for total uncorrected exposure times of ~ 22 ks & 18 ks (epoch I) and ~ 58 ks & 37 ks (epoch II) for the XIS and HXD detectors respectively.

All data reduction and analysis takes place within the HEASOFT 6.6.1 environment, which includes FTOOLS 6.6, SUZAKU 11 and XSPEC 12.5.0. The latest versions of the relevant *Suzaku* CALDB files were also used.

Electronic address: markrey@umich.edu

¹ Department of Astronomy, University of Michigan, 500 Church Street, Ann Arbor, MI 48109

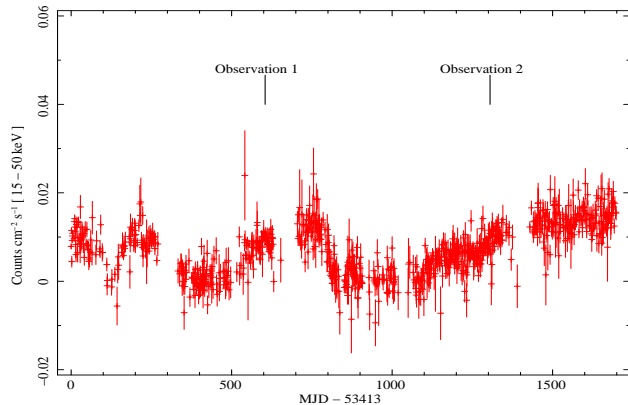


FIG. 1.— *Swift* BAT hard X-ray lightcurve for 1E 1740.7-2942 from May 2005 to Jan 2009, only exposures greater than 1ks are plotted. The times of the *Suzaku* observations presented in this paper are indicated.

2.1. X-ray Imaging Spectrometer

The XIS has a field of view of $\sim 18' \times 18'$ (1024^2 pixels) and was operated in 5x5 and 3x3 readout mode. In addition the data was taken in full window mode providing a time resolution of 8 seconds. The raw data were processed following standard procedures, for details see *Suzaku* abc guide². Photon pile-up was not an issue during these observations, so a circular extraction region of radius 250 pixels was utilized (250 pixels is the recommended radius to extract $\sim 99\%$ of a point source flux). In both observations 1E 1740.7-2942 is located close to the edge of the detector, hence our extraction region is the intersection of the detector edge and the circular aperture. The resultant extraction region has an effective area equivalent to $\sim 95\%$ of the 250 pixel radius, and hence we expect to have detected a commensurate percentage of the total source flux in the soft X-ray band (< 10 keV). Background spectra were extracted from a neighbouring region of the detector, Response files were generated using the tasks XISRMFGEN and XISSIMARFGEN. The background and response files were then grouped with the science spectrum for analysis in XSPEC.

2.2. Hard X-Ray Detector

The HXD covers the energy range from 10 – 600 keV, consisting of two separate detectors, (i) PIN: Silicon PIN photodiodes covering the energy range 10 – 70 keV and, (ii) GSO: GSO/BGO phoswich scintillators covering the energy range 40 – 600 keV. This instrument has a $35' \times 35'$ field of view (FoV) at energies below 100 keV, while above this the FoV is $\sim 4.5^\circ \times 4.5^\circ$. As the time of writing, the GSO data processing routines had not been included in the official *Suzaku* data reduction pipeline, all of the hard X-ray detector data was reprocessed following the prescription in the abc-guide², see also Reynolds et al. (2010) for a detailed description of the PIN/GSO extraction procedure.

3. ANALYSIS & RESULTS

3.1. Soft X-ray Background

X-ray observations of the Galactic center have revealed a diffuse X-ray emission component, the Galactic center diffuse X-ray emission (GCDX, e.g. Koyama et al. 2007b,c). Observations with *Suzaku* have revealed this emission to be consistent with emission from a collisionally ionized plasma with a temperature of 5 – 7 keV. A number of distinct atomic emission lines have been observed from this plasma. In particular, emission from the Iron lines Fe I $K\alpha$, Fe XXV $K\alpha$, Fe XXVI $K\alpha$ has been resolved (Koyama et al. 2007c). As such, it is important that we account for any contamination from the GCDX in our 1E 1740.7-2942 spectrum.

In Fig. 3, we plot the background spectrum extracted from the 1E 1740.7-2942 epoch II spectra. Here due to the different sensitivities of the front illuminated (XIS1) and back illuminated (XIS0, XIS3) detectors in the XIS, we use the data from XIS1 for the low energy band (< 5 keV) and the data from XIS0, XIS3 above this. A number of lines from the GCDX are clearly detected, the line parameters are listed in Table 1. The ratio of the fluxes for the Fe-lines are consistent with those measured towards the Galactic center (Yamauchi et al. 2008).

3.2. Broadband Spectra

As the extinction is high, we do not detect any significant flux below 2 keV in either epoch. In Fig. 2, we plot the spectra extracted from the epoch II data along with their associated background spectra. Assuming that the systematics in the GSO background are understood at the $< 2\%$ level (Fukazawa et al. 2009), 1E 1740.7-2942 is detected out to ~ 300 keV. For reference, at a systematic level of 3% the flux from 1E 1740.7-2942 is equal to that of the background at 300 keV.

1E 1740.7-2942 resides in a crowded region of the Galactic plane; as such, it is important to check for contamination from nearby sources. Fortunately, the Galactic center was, and continues to be, observed by *INTEGRAL*, as part of the Galactic bulge monitoring program³, e.g. Kuulkers et al. 2007. This area was observed within a couple of days of the *Suzaku* observations presented in this paper (Revolution #488, #721), and these observations provide us with flux measurements for other sources that were bright at hard X-ray energies during our observations.

On both occasions 1E 1740.7-2942 was the dominant bright hard X-ray source in this field. The nearest bright hard X-ray source, 1A 1742-294, was active during the first observation only. However, this system lies $31'$ from 1E 1740.7-2942, which was approximately centered in the HXD FoV, and hence lay outside our FoV during the observations presented in this paper. As such, below 100 keV we only detect flux from 1E 1740.7-2942. We are unable to rule out the presence of contaminating flux above this energy as there are a number of hard X-ray sources in the large $4.5^\circ \times 4.5^\circ$ FoV. We note that the consistency between the model normalizations for the PIN & GSO spectra would argue against the presence of a significant contaminating flux above 100 keV.

Our final good spectral range is XIS0, XIS3: 2 – 10 keV, XIS1: 2 – 10 keV, PIN: 12 – 70 keV, and GSO: 50 – 300 keV. Additionally the data were rebinned prior to fitting in XSPEC with the ftool GRPPHA by a factors of 4

² <http://heasarc.gsfc.nasa.gov/docs/suzaku/analysis/abc/>

³ <http://isdc.unige.ch/Science/BULGE/>

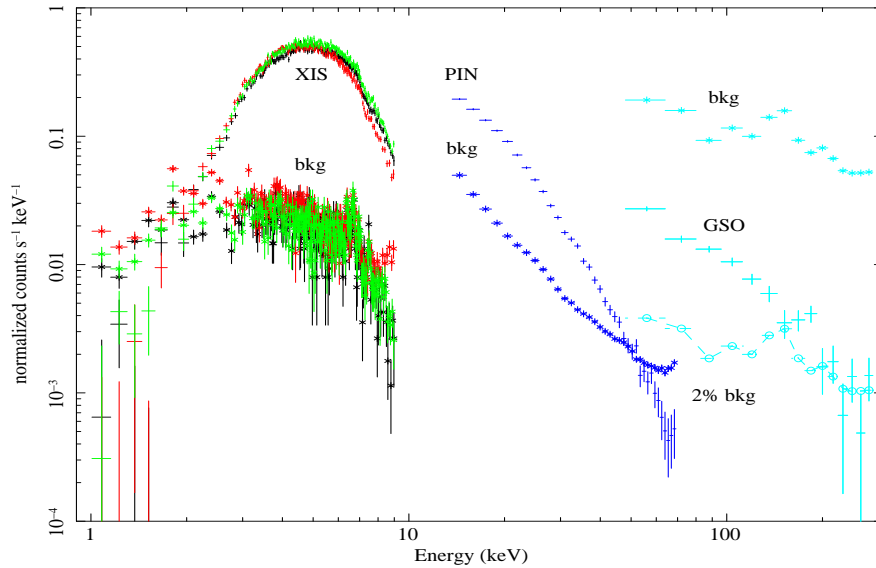


FIG. 2.— Background subtracted XIS, PIN and GSO spectra and their associated background spectra. 1E 1740.7-2942 is detected between 2 – 300 keV, with the low energy cutoff due to the high column density towards this source. The XIS detects the source between energies of 2 – 10 keV, the PIN detects it out to 70 keV, while the GSO detects flux to ~ 300 keV assuming the background is reproducible to an accuracy of $<2\%$ (see text).

and 8 for the XIS/PIN & GSO spectra respectively. As the S/N in the second epoch is higher, we focus on these spectra. The results for the fits to the data from epoch I, which are similar to those from epoch II, are presented in Table 2.

3.2.1. Power-law models

The resultant spectrum (2 - 300 keV) was initially fit with a model consisting of a power-law modified by interstellar extinction (i.e. `pha*po`). The fit is found to be a poor one ($\chi^2_\nu \sim 1.45$) with large residuals present at higher energies. To account for these residuals, we considered 2 additional power-law models; a model with a cutoff at high energies (`cutoffpl`) and a broken power-law (`bknpo`). The `cutoffpl` provides a significant improvement over the power-law model alone $\chi^2_\nu \sim 1.16$, with the cutoff energy found to be ~ 150 keV (epoch II). The broken power-law provides the best fit to the data $\chi^2_\nu \sim 1.04$, with the spectrum observed to break from a very hard power-law, $\Gamma \sim 1.4$, to a softer power-law, $\Gamma \sim 1.8$, at an energy of approximately 7 keV. This clearly points towards a second component at low energies in the observed spectrum, with the most obvious culprit being thermal emission from a geometrically thin optically thick accretion disc (Shakura & Sunyaev 1973), see Table 2 for the detailed fit model parameters.

Inspection of the residuals from this model reveals a number of features in the XIS spectral range. At low energies (2 – 3 keV), there remains a feature consistent with the expected position of the S XV line (2.45 keV), in addition to the presence of known systematic features in the 2.1 – 2.4 keV region. At energies 9 - 10 keV there is an unidentified residual (in the form of an excess possibly due to the background although its actual origin is unclear), as such in all further modelling both of these regions are ignored.

A large residual also exists at energies above the iron K absorption edge ($E = 7.11$ keV). It is clear that we must accurately account for this spectral feature. To

do this we use the variable iron abundance absorption model available in `XSPEC - zvfeabs`. The absorption edge energy was frozen at 7.11 keV (allowing it to vary does not significantly improve the fit). As there exists a degeneracy in this model between the Hydrogen column density and the metal/iron abundance, N_H was frozen at a value of $1 \times 10^{23} \text{ cm}^{-2}$ in agreement with the previously determined *Chandra* value (Gallo & Fender 2002).

A blackbody accretion disc was now added to the power-law models above (e.g. `zvfeabs*(diskbb+po)`) and the fitting was repeated. The resulting fit is significantly improved and is equal to the broken power-law model, see Table 2. In this case there is no difference between the cutoff power-law and power-law models. However, the cutoff energy for both epochs pegs at the `XSPEC` hard limit of 500 keV, formally we find a lower limit for the cutoff energy of ~ 340 keV & ~ 390 keV at the 90% confidence level in epochs I & II respectively. It is rare that spectral breaks are restricted to such high energies in the low-hard state and this may be related to the fact that some models require only a small seed photon fraction to fit the data. The accretion disc is found to have a temperature of ~ 0.4 keV, while the disc normalization points towards a small inner radius for the accretion disc. The metal abundance is found to be high in agreement with previous *ASCA* observations where the iron abundance was measured to be $\sim 2x$ solar (Sakano et al. 1999). We find an iron abundance of $N_{\text{Fe}} = 1.7 \pm 0.15$ and a metals abundance of $N_Z = 1.95 \pm 0.15$ relative to solar abundances.

The disc normalization may be used to estimate the inner radius of the accretion disc when knowledge of the distance and inclination are available, as $\text{norm} \sim (r_{\text{in}}/d_{10 \text{ kpc}})^2 \cos \theta$. This estimate is subject to a number of well known corrections, e.g. spectral hardening (Shimura & Takahara 1995), inner radius (Makishima et al. 2000) and a number of others which are difficult to quantify, e.g. zero torque inner boundary condition (Zimmerman et al. 2005) and radia-

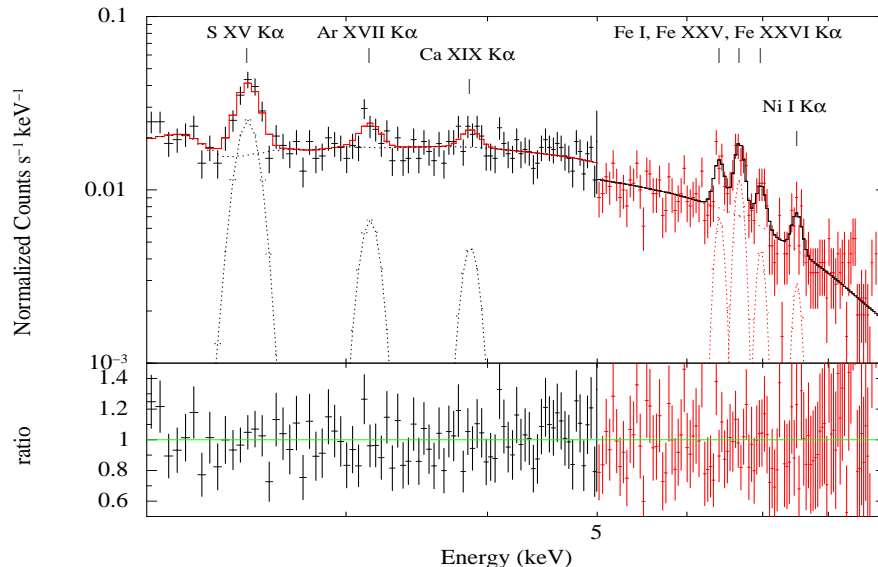


FIG. 3.— Spectrum of the soft X-ray background towards 1E 1740.7-2942. XIS1 data is displayed below 5 keV (black), with data from XIS3 displayed above 5 keV (red). A number of prominent emission lines are clearly detected (see text & Table 1).

tive transfer effects (Merloni et al. 2000). Assuming a distance of 8.5 kpc, we measure an inner radius of $\sim 250 (\cos i^{-1} d_{8.5\text{kpc}})$ km and $\sim 120 (\cos i^{-1} d_{8.5\text{kpc}})$ km for epochs I & II respectively assuming a power-law continuum (see Table 2). We note that the ISCO for a Schwarzschild (Kerr) black hole is 6 (1.23) R_g , for a 10 M_\odot black hole this is equivalent to a radius of 90 (15) km. The inclination of 1E 1740.7-2942 is unconstrained; however, the presence of a bi-polar radio jet (Mirabel et al. 1992) would suggest a high inclination. For instance an inclination angle of 70° , will result in an increase in the inner radii above by a factor of 3. Nonetheless the inner radii measured here are consistent with being close to the ISCO, i.e. $R_{\text{in}} \lesssim 20 R_g$.

We test for the presence of a broad iron line by adding a **laor** component to the model, whose energy is restricted to the 6.4 – 6.97 keV range ($q = 3$, $R_{\text{out}} = 400$, $i = 70^\circ$). The presence of a broad line ($E \sim 6.7\text{keV}$, $R_{\text{in}} \sim 3 R_g$) is only marginally required (99% confidence level as measured with an F-test). As such we freeze the inner radius at $3 R_g$ and step the line energy through the energy region outlined above. For a relativistic line centered at 6.4 keV, we can place an upper limit in the EW of this line of ~ 60 eV, for higher energies, e.g. 6.7, 6.9 keV the upper limit increases to ~ 150 , 200 eV respectively.

Likewise in order to investigate the possible contribution due to disc reflection at higher energies (20 – 40 keV), the best fit power-law from above was convolved with the reflection model of Magdziarz & Zdziarski (1995) **reflect*po**. This model was then relativistically blurred (**kdblur**) to account for the proximity of the accretion disc to the ISCO as indicated above. The inclination was held fixed ($\cos i = 0.45$), while the abundances of metals were tied to those of the absorption component. Any reflection fraction is negligible ($f \sim 1\%$). Formally, we find an upper limit for disc reflection of 10% at the 90% confidence level.

Ueda et al. (2009) have detected numerous absorption lines, in particular Fe XXV, XXVI, attributed to a disc

wind in soft state observations of the microquasar GRS 1915+105. Earlier hard state observations by Lee et al. (2002) had also detected some of these lines; however, they were significantly weaker. Here we test for the presence of narrow Gaussian absorption lines in the Fe region of the spectrum. No significant absorption lines are detected, at the 90% confidence level we place an upper limit on the equivalent width of any absorption line of < 3 eV.

We note that due to the higher S/N in the second epochs data, this fit provides tighter spectral constraints, which nonetheless are consistent with those from epoch I within the errors.

3.2.2. Comptonization models

To investigate the Comptonizing medium/region, we use the bulk motion Comptonization model – **bmc** (Titarchuk et al. 1997). This is a generic Comptonization model which includes the flux from the accretion disc and the fraction of this seed flux Comptonized in the corona. We use this model as it considers the general case where the Comptonization process may be either thermal or dynamic in nature⁴. In the **bmc** model the soft photons are those that undergo few scatterings, while those in the hard component have undergone multiple scatterings.

Our fit results in a reduced chi-squared of ~ 1.04 (1327/1272 – epoch II, 1297/1272 – epoch I, see Fig. 4), with the best fit parameters consistent with those found in the previous section. The temperature of the soft disc component for epoch II (I) is 0.36 ± 0.02 keV (0.28 ± 0.06 keV). The spectral index α agrees with our expectations from the **diskbb+po** fit, i.e. $\Gamma = 1.79 \pm 0.03$ (1.82 ± 0.04) where $\alpha = \Gamma - 1$, while $A = -0.62 \pm 0.09$ ($-0.82^{+0.46}_{-0.17}$). We find both iron and metals to be over abundant relative to solar ($\sim 2x$, $1.7x$ respectively).

Testing for the presence of a relativistic iron line re-

⁴ In the thermal Comptonization case, for energies less than $\sim 2kT_e$, the **comptt** & **bmc** models are similar.

TABLE 1
2 - 10 keV BACKGROUND FEATURES

K α Line	Energy [keV]	EW [eV]
S XV	2.45 \pm 0.01	240 $^{+400}_{-100}$
Ar XVII	3.15 \pm 0.03	65 $^{+250}$
Ca XIX	3.86 \pm 0.06	48 $^{+70}$
Fe I	6.41 \pm 0.02	100 $^{+200}_{-70}$
Fe XXV	6.68 \pm 0.02	200 $^{+200}_{-130}$
Fe XXVI	6.98 \pm 0.3	90 $^{+200}$
Ni I	7.51 \pm 0.05	120 $^{+200}$

NOTE. — Atomic lines detected in the 1E 1740.7-2942 background spectrum. All errors are quoted at the 90% confidence level. Note: where lower limits are not given, the lower limit is consistent with zero.

veals results consistent with those in the previous section. We also attempted to constrain the possible presence of non-thermal electrons at higher energies using the hybrid Comptonization model *eqpair* (Coppi 2000); however, we are unable to constrain the fraction of non-thermal/thermal electrons. As discussed in Coppi (2000), this is unsurprising as in order to constrain the non-thermal fraction, one requires a source detection out to energies approaching 500 keV.

4. DISCUSSION

We present *Suzaku* broadband spectra of the Galactic microquasar 1E 1740.7-2942 while in the low-hard state. The source was observed on two separate occasions after a transition from the high-soft state to the low-hard state at a luminosity of $\sim 1\%$ Eddington, i.e. a 2 - 300 keV unabsorbed flux of 2.2×10^{-9} erg s $^{-1}$ cm $^{-2}$ ($L_x/L_{\text{Edd}} = 0.014 \times (d/8.5 \text{ kpc})^2 (M_x/10 M_\odot)$).

Given the large background at energies above 200 keV, it is worth investigating the effect of ignoring data beyond this, and how this might affect the presence of a spectral cut-off in our data. Ignoring all data in excess of 200 keV and refitting the higher quality epoch II data does not significantly change our results, with a lower limit to the spectral cutoff of ~ 375 keV (90% confidence) in this case. We note, that the best fit cut-off power-law model, where the spectral cut-off is fixed at an energy of 200 keV, is excluded at the $> 3\sigma$ & $> 4\sigma$ level, as measured via a F-test, for epochs I & II respectively, see Table 2

The observed low-hard state spectrum of 1E 1740.7-2942 as presented herein, and via the *INTEGRAL* observations presented by Bouchet et al. (2009), is clearly consistent with a power-law. Here 1E 1740.7-2942 is detected up to an energy of 300 keV. A prominent iron K absorption edge is visible in the XIS soft X-ray spectra. We account for this with the *zvfabs* model in XSPEC and find the metal & iron abundances to be super-solar for all our models in agreement with previous *ASCA* observations (Sakano et al. 1999). Modeling the spectrum as the sum of a blackbody accretion disc and an unbroken power-law at higher energies provides a good fit, although we can not rule out the presence of a spectral cut off at energies $\gtrsim 380$ keV.

The accretion disc temperature is determined to be low (~ 0.4 keV), while we find the disc inner radius to be small and consistent with a disc that is continuous down

to small radii approaching the ISCO (i.e. $R_{\text{in}} \lesssim 20 R_g$; see Table 2). A broad iron line is also required but at a low significance (99% as measured by an F-test), supporting a small inner radius for the accretion disc. The detection of a cool disk in 1E 1740.7-2942 is consistent with a growing body of evidence that the accretion disk is not necessarily truncated at large radii in the low-hard state.

The spectrum is characterized in detail using the *bmc* Comptonization model (Titarchuk et al. 1997). A cool source of thermal photons is revealed in this model consistent with the presence of a cool accretion disc, as suggested by the phenomenological modelling above. The parameter $\log(A)$ in the *bmc* model is related to the fraction of Comptonized soft seed photons $f = A/(1 + A)$, in these observations the fraction is low. In epoch II the Comptonized fraction is $\sim 20\%$ while in epoch I it is lower still at 15%. Unfortunately the lower S/N in epoch I prevents us from making any definitive statements regarding the evolution of the coronal geometry between observations.

4.1. Previous Observations

Bouchet et al. (2009) have observed this system with *INTEGRAL* in the hard state, and detect it out to an energy of 600 keV. The spectrum is found to be consistent with thermal Comptonization up to 200 keV with an additional component required at energies above this. They fit the spectrum with a two component thermal Comptonization model ($kT_{e1} \sim 30$ keV, $kT_{e2} \sim 100$ keV) although they are unable to rule out non-thermal processes. Indeed fitting the spectrum above 200 keV with a power-law produces a high quality fit ($\chi^2_\nu \sim 1$). Such a power-law could be produced by non-thermal processes such as those expected from a jet, e.g. Markoff et al. (2004). The measurement of a power-law spectrum for 1E 1740.7-2942 out to 600 keV by *INTEGRAL* is consistent with the *Suzaku* observations presented herein.

Del Santo et al. (2005) carried out a series of simultaneous *RXTE* & *INTEGRAL* observations primarily while 1E 1740.7-2942 was in the low-hard state. The spectrum was found to be consistent with a power-law ($\Gamma \sim 1.3 - 1.6$) including a high energy cut-off ($\sim 100 - 120$ keV); however, we note that the S/N of the high energy (> 50 keV) portion of the spectrum is very low, with only a single data bin at > 100 keV. A significant amount of reflection from the accretion disc was also required, with typical values for the reflection fraction of 0.3 - 0.9. Fitting with the *compps* model reveals a seed photon temperature of 0.4 - 0.7 keV, consistent with the accretion disc temperature we measure here.

We do not observe any high energy cut-off features, as observed by Del Santo et al. (2005), in our data. Although, we note the power-law emission is clearly softer in our case ($\Gamma \sim 1.8$). We do not observe any evidence for significant disc reflection (either an iron line or Compton hump) in the spectra from either epoch, with a detection of a weak line at the 99% confidence level (EW ~ 60 eV) in addition to a weak disk reflection fraction ($f \lesssim 0.1$). Given the high level of Comptonization clearly present, it is likely that any fluorescent iron line emission produced in the inner disc would be smeared by the corona (Petrucchi et al. 2001). The lack of these features is consistent with the expectation of a radially re-

TABLE 2
SPECTRAL FIT PARAMETERS

Model	Epoch	N_Z [N_{Z_\odot}]	N_{Fe} [N_{Fe_\odot}]	Γ_1	Γ_2	E_{cut} [keV]	E_{break} [keV]	χ^2/ν
po	I	1.36±0.06	1.55±0.20	1.74±0.04	—	—	—	1335.91/1274
po	II	1.44±0.04	1.29±0.13	1.67±0.02	—	—	—	1538.04/1274
cutoffpl	I	1.31 $^{+0.07}_{-0.08}$	1.63±0.22	1.68 $^{+0.04}_{-0.07}$	—	—	335 $^{>500}_{-160}$	1332.85/1273
cutoffpl	II	1.30±0.05	1.51±0.14	1.52±0.04	—	—	143 $^{+44}_{-28}$	1473.81/1269
bknpo	I	1.06±0.10	1.34±0.22	1.27 $^{+0.13}_{-0.08}$	1.79±0.04	—	6.0±0.3	1293.43/1272
bknpo	II	0.99±0.06	1.99±0.15	1.29±0.05	1.79±0.03	—	7.7±0.2	1327.99/1272

Model	Epoch	N_Z [N_{Z_\odot}]	N_Z N_{Fe_\odot}	T_{bb} [keV]	XIS1 _{norm}	R_{in} [km]	Γ [keV]	E_{cut} [keV]	χ^2/ν
diskbb+po	I	1.58±0.11	1.67±0.22	0.32±0.08	21230 $^{+7.1e5}_{-18219}$	248 $^{+1205}_{-154}$	1.82±0.04	—	1292/1270
diskbb+po	II	1.98±0.10	1.70±0.15	0.41±0.02	4696 $^{+2206}_{-1442}$	117 $^{+24}_{-20}$	1.77±0.03	—	1317/1270
diskbb+cutoffpl	I	1.51 $^{+0.12}_{-0.10}$	1.70±0.22	0.30±0.09	26707 $^{+1.9e6}_{-24111}$	278 $^{+2082}_{-190}$	1.77±0.04	> 343	1296/1269
diskbb+cutoffpl	II	1.89±0.10	1.72±0.15	0.41±0.02	3537 $^{+1937}_{-1165}$	101 $^{+25}_{-18}$	1.74±0.03	> 389	1320/1269

Model	Epoch	N_Z [N_{Z_\odot}]	N_{Fe} [N_{Fe_\odot}]	kT [keV]	α	log(A)	χ^2/ν
bmc	I	1.58 $^{+0.12}_{-0.10}$	1.67±0.21	0.28 $^{+0.06}_{-0.04}$	0.82±0.04	-0.82 $^{+0.46}_{-0.99}$	1297/1272
bmc	II	1.95±0.1	1.69±0.15	0.36±0.02	0.79±0.03	-0.62±0.09	1327/1272

NOTE. — The Hydrogen column density was frozen at a value of $1 \times 10^{23} \text{ cm}^{-2}$ in agreement with previous estimates (Gallo & Fender 2002). The iron absorption edge energy was also fixed at 7.11 keV. Errors quoted are 90% confidence intervals determined via the **error** command in XSPEC. The accretion disc inner radius is calculated assuming a distance of 8.5 kpc, additionally the inclination dependence of $(\cos i)^{-1}$ has not been included.

cessed/truncated disc in the hard state (Gierlinski et al. 1997) and/or the presence of an outflow (Beloborodov 1999; Merloni & Fabian 2002; Markoff & Nowak 2004).

Observations of 1E 1740.7-2942 with *Chandra* also measure a hard power-law spectrum consistent with the expectations for the hard state $\Gamma \sim 1.4$ (Gallo & Fender 2002). We note that a power-law fit to our *Suzaku* spectrum in the 2 – 10 keV range also returns a photon index of ~ 1.4 suggesting that the *Chandra* spectrum contained a significant accretion disc component, which is only revealed through the broad energy coverage of *Suzaku*.

The observations listed above are in agreement with those presented in this paper, and point towards the X-ray emission from 1E 1740.7-2942 being dominated by the accretion disc & corona while the source is in the LHS. This interpretation is supported by the work of (Bosch-Ramon et al. 2006) who modelled the broadband emission (radio - GeV) from 1E 1740.7-2942. They find the observed hard X-ray flux to be inconsistent with the measured radio flux in the case where the spectral energy distribution is jet dominated and instead favour the corona as the origin of the observed high energy emission.

4.2. Implications for the low-hard state

Observations of the candidate black hole binary SWIFT J1753.5-0127 in the low-hard state with *Suzaku* reveal a similar picture (Reynolds et al. 2010), i.e. a low temperature accretion disc component plus an unbroken power-law extending to high energies at a luminosity of $\sim 2\% L_{Edd}$. In this case the disc temperature is found to be ~ 0.2 keV while the inner radius is consistent with that measured for 1E 1740.7-2942. A low reflection fraction of ~ 0.2 is measured along with an unbroken power-law and a weak iron line,

all consistent with an inner radius $\lesssim 20 R_g$. A similar picture is revealed through modelling the soft disc component and the relativistic iron line detected by *XMM* (Miller et al. 2006a; Hiemstra et al. 2009). The low values measured for the reflection fraction in both 1E 1740.7-2942 and SWIFT J1753.5-0127 are consistent with models that do not require a recessed disc in the low-hard state, e.g. Beloborodov (1999); Merloni & Fabian (2002); Markoff & Nowak (2004).

Combined with the accretion disc component and relativistically broadened iron lines observed in numerous systems, these results provide significant evidence opposing the view that the accretion disc is truncated at large radii ($> 100 R_g$) in the low-hard state, e.g., see also Miller et al. (2006b); Tomsick et al. (2008); Wilkinson & Uttley (2009); Reis et al. (2009, 2010).

4.3. Comparison to other Microquasars

GRS 1758-258 is the system most closely resembling 1E 1740.7-2942 among the Galactic black hole candidates. However, we first consider a series of broadband observations of the black hole binaries XTE J1650-500 and GRO J1655-40, which displayed low-hard state spectra similar to that presented in this paper for 1E 1740.7-2942.

XTE J1650-500 is a Galactic black hole binary that was discovered in 2001 by *RXTE* (Remillard 2001). The orbital period has been measured to be ~ 7.6 hrs, and the mass of the black hole is $M_{BH} = 4.0 - 7.3 M_\odot$ (Orosz et al. 2004). Observations during the initial outburst with *XMM-Newton* detected a broad skewed Fe-K α , which modelling revealed to be consistent with a near maximally spinning black hole ($a^* \sim 1$; Miller et al. 2004). Observations at radio wavelengths revealed significant emission consistent with a origin in a com-

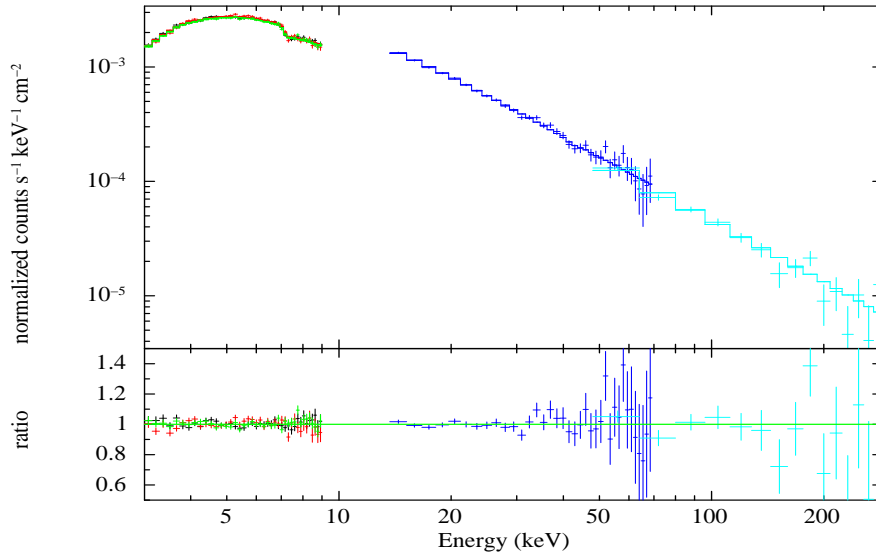


FIG. 4.— Best fit to the epoch II spectrum, consisting of Comptonization modified by absorption with a variable iron abundance, *zvfabs*bmc*: $\chi^2_\nu \sim 1.04$. The thermal component temperature is ~ 0.36 keV, and the photon index is ~ 1.8 , see Table 2. The XIS0, XIS1, XIS2 spectra are indicated by the black, red and green points respectively, while the PIN (blue) and GSO (light blue) are also plotted.

pact jet (Corbel 2004). Montanari et al. (2009) analyze *BeppoSax* observations of XTE J1650-500 with the *bmc* model⁵ in the the low-hard and high-soft states. The photon index in the low-hard state is similar to our observations $\Gamma \sim 1.7 - 1.8$. The soft seed component is found to have a temperature of ~ 0.4 keV again similar to our observations of 1E 1740.7-2942. In contrast to XTE J1650-500, we find a much lower Comptonized fraction in the case of 1E 1740.7-2942 $\sim 20\%$ (versus $\sim 60\%$), which implies a smaller corona. In the case of XTE J1650-500, Montanari et al. (2009) find evidence for a contraction in the size of the Corona as the microquasar transitions from the LH to the HS state, as such one might naturally expect the corona to be smaller when the transition progresses in the opposite sense.

GRO J1655-40 was discovered by the *Compton Gamma Ray Observatory* in 1994 (Zhang et al. 1994) and found to lie at a distance of ~ 3.2 kpc (Tingay et al. 1995). Orosz & Bailyn (1997) measured an orbital period of ~ 2.6 days and the black hole mass to be $M_x = 7.02 \pm 0.22 M_\odot$. Highly relativistic radio jets were also detected, which appeared to be misaligned with the binary orbit (Hjellming & Rupen 1995). X-ray observations revealed a pair of high frequency QPOs consistent with Keplerian rotation at the ISCO of a spinning black hole (Strohmayer 2001). Subsequent observations detected a broadly skewed iron $K\alpha$ line, which supports a high spin for the black hole ($a \geq 0.9$; Miller et al. 2005, 2009). Tomsick et al. (1999) presented *RXTE* and *OSSE* observations in the high-soft state which revealed unbroken power-law emission out to an energy of ~ 800 keV. Caballero Garcia et al. (2007) presented broadband (3 – 500 keV) *INTEGRAL* observations of GRO J1655-40 during the 2005 outburst. Here an observation in the low-hard state ($L_x \sim 0.015 L_{\text{Edd}}$) clearly detected unbroken

power-law emission ($\Gamma \sim 1.7$) extending out to an energy of ~ 500 keV, again consistent with the observations of 1E 1740.7-2942 presented herein. This was interpreted as evidence for a significant contribution from non-thermal electrons (although, see also Joinet et al. 2008). Unfortunately, the *INTEGRAL* low energy cut-off of 3 keV does not allow any constraints to be placed on emission from the accretion disc.

GRS 1758-258 is the second persistent microquasar to lie close to the Galactic center. It is similar to 1E 1740.7-2942, i.e. large scale radio outflows (Rodriguez et al. 1992), X-ray bright with a high extinction (Sunyaev et al. 1991), no identified optical/NIR counterpart (Eikenberry et al. 2001) and a long orbital period (~ 18.5 days; Smith et al. 2002). Detailed studies of the LHS state properties of this system have been carried out by Pottschmidt et al. (2006) and Sidoli & Mereghetti (2002) who observed with *INTEGRAL/RXTE* & *BeppoSax* respectively. Pottschmidt et al. (2006) detected the source in the energy range 3 – 200 keV and found the low-hard state spectrum to be consistent with a cut-off power-law, where $\Gamma \sim 1.5 - 1.7$ and $E_{\text{cut}} \sim 140 - 250$ keV. Due to contamination from GX 5-1, Sidoli & Mereghetti (2002) only detected GRS 1758-258 in the energy ranges 0.1 – 10 keV & 40 – 200 keV and found the broadband spectrum to be consistent with a cut-off power-law where $\Gamma \sim 1.65$, $E_{\text{cut}} \sim 70$ keV and $E_{\text{fold}} \sim 180$ keV. In both sets of observations a weak emission line consistent with Fe- $K\alpha$ was marginally detected with an equivalent width $\sim 50 - 70$ eV. New broadband *Suzaku* observations of GRS 1758-258 will be presented in an upcoming paper (Reynolds et al., 2010 in prep.).

5. CONCLUSIONS

We present *Suzaku* observations of the Galactic center microquasar 1E 1740.7-2942 in two separate epochs taken after the system had transitioned into the low-hard state. The system is observed to be in the low-hard state at the time of our observations with an X-ray luminos-

⁵ Montanari et al. (2009) also include an extra blackbody component to account for that portion of the disc that is not covered by the corona, as we do not detect any photons below 2 keV this component is not required.

ity of $\sim 1\%$ Eddington. The spectra in each epoch are similar, being described by a model consisting of a soft thermal accretion disc component ($T \sim 0.4$ keV) and the broadband emission (> 10 keV) is found to be characterized by an unbroken power-law to at least 300 keV.

Consistent with growing evidence from observations of numerous systems in the low-hard state (e.g. GX 339-4, SWIFT J1753.5-0127, XTE J1817-330, XTE J1118+480), we also find evidence that the accretion disc in 1E 1740.7-2942 is not truncated at large radii in the low-hard state and instead resides close to the ISCO

($R_{\text{in}} \sim 20 R_g$).

We thank the anonymous referee for his/her careful review and report. This research has made use of data obtained from the *Suzaku* satellite, a collaborative mission between the space agencies of Japan (JAXA) and the USA (NASA). This research made extensive use of the *SIMBAD* database, operated at CDS, Strasbourg, France and NASA's Astrophysics Data System.

REFERENCES

- Beloborodov A. 1999, ApJ, 510, 123
 Bouchet L., Del Santo M., Jourdain E., Roques J.P., Bazzano A., De Cesare G., 2009, ApJ, 693, 1871
 Bosch-Ramon V., Romero G.E., Paredas J.M., Bazzano A., Del Santo M., Bassani L., 2006, A&A, 457, 1011
 Caballero-Garcia M.D., Miller J.M., Kuulkers E. et al., 2007, ApJ, 669, 534
 Castro-Tirado A.J., Brandt S., Lund N., 1992, IAUC, 5590, 2
 Coppi P.S., 2000, HEAD, 5, 2311
 Corbel S., Fender R.P., Tomsick J.A., Tzioumis A.K., Tingay S., 2004, ApJ, 617, 1272
 Del Santo M., Bazzano A., Zdziarski A.A. et al., 2005, A&A, 433, 613
 Eikenberry S.S., Fischer W.J., Egami E., Djorgovski S.G., 2001, ApJ, 556, 1
 Fukazawa Y., Mizuno T., Takahashi H. et al., 2009, PASJ, 61, 17
 Gallo E., Fender R.P., 2002, MNRAS, 337, 869
 Gierlinski M., Zdziarski A.A., Done C., Johnson W.N., Ebisawa K., Ueda Y., Haardt F., Phillips B.F., 1997, MNRAS, 288, 958
 Heidl W.A., Prince T.A., Grunsfeld J.M., 1994, ApJ, 430, 829
 Hertz P., Grindlay J.E., 1984, ApJ, 278, 137
 Hiemstra B., Soleri P., Mendez M., Belloni T., Mostafa R., Wijnands R., 2009, MNRAS, 394, 2080
 Hjellming R.M., Rupen M.P., 1995, Nature, 375, 464
 Joinet A., Kalemci E., Senziani F., 2008, ApJ, 679, 655
 Kokubun M., Makishima K., Takahashi T. et al., 2007, PASJ, 59, 53
 Koyama K., Tsunemi H., Dotani T. et al., 2007a, PASJ, 59, 23
 Koyama K., Uchiyama H., Hyodo Y. et al., 2007b, PASJ, 59, 237
 Koyama K., Hyodo Y., Inui T. et al., 2007c, PASJ, 59, 245
 Kuulkers E., Shaw S.E., Paizis A. et al., 2007, A&A, 466, 595
 Lee J.C., Reynolds C.S., Remillard R., Schulz N.S., Blackman E.G., Fabian A.C., 2002, ApJ, 567, 1102
 Magdziarz P., Zdziarski A.A., 1995, MNRAS, 273, 837
 Makishima K., Kubota A., Mizuno T. et al., 2000, ApJ, 535, 632
 Markoff S., Nowak M., Corbel S., Fender R., Falcke H., 2003, A&A, 397, 645
 Markoff S., Nowak M., 2004, ApJ, 609, 272
 Marti J., Mirabel I.F., Chaty S., Rodriguez L.F., 2000, A&A, 363, 184
 McClintock J.E., Remillard R.A., 2006, in Lewin W.H.G., van der Klis M., eds, Compact Stellar X-Ray Sources, Cambridge University Press, Cambridge, in press (astro-ph/0306213)
 Merloni A., Fabian A.C., Ross R.R., 2000, MNRAS, 313, 193
 Merloni A., Fabian, A. 2002, MNRAS, 332, 165
 Miller J.M., Fabian A.C., Wijnands R. et al., 2004, ApJ, 570, 69
 Miller J.M., Fabian A.C., Nowak M.A., Lewin W.H.G., 2005, in Proc. 10th Marcel Grossmann Meeting on General Relativity, ed., Novello M., Bergliaffa P. (Hackensack: World Sci.), 1296
 Miller J.M., Homan J., Miniutti G., 2006a, ApJ, 652, 113
 Miller J.M., Homan J., Steeghs D., Rupen M., Hunstead R.W., Wijnands R., Charles P.A., Fabian A.C., 2006b, ApJ, 653, 525
 Miller J.M., Reynolds C.S., Fabian A.C., Miniutti G., Gallo L.C., 2009, ApJ, 697, 900
 Mirabel I.F., Rodriguez L.F., Cordier B., Paul J., Lebrun F., 1992, Nature, 358, 215
 Mirabel I.F., Rodriguez L.F., 1994, Nature, 371, 46
 Mirabel I.F., Rodriguez L.F., 1999, ARA&A, 37, 409
 Mitsuda K. et al., 2007, PASJ, 59, 1
 Montanari E., Titarchuk L., Frontera F., 2009, ApJ, 692, 1597
 Orosz J.A., Bailyn C.D., 1997, ApJ, 477, 876 (erratum: 1997, ApJ, 482, 1086)
 Orosz J.A., McClintock J.E., Remillard R.E., Corbel S., 2004, ApJ, 616, 376
 Petrucci P.O., Merloni A., Fabian A., Haardt F., Gallo E., 2001, MNRAS, 328, 501
 Pottschmidt K., Cherny M., Zdziarski A.A., Lubinski P., Smith D.M., Bezayiff N., 2006, A&A, 452, 285
 Reis R.C., Fabian A.C., Ross R.R., Miller J.M., 2009, MNRAS, 395, 1257
 Reis R.C., Fabian A.C., Miller J.M., 2010, MNRAS, 402, 836
 Remillard R.A., 2001, IAUC, 7715
 Reynolds M.T., Miller J.M., Homan J., Miniutti G., 2010, ApJ, 709, 358
 Rodriguez L.F., Mirabel F., Marti J., 1992, ApJ, 401, 15
 Sakano M., Imanishi K., Tsujimoto M., Koyama K., 1999, ApJ, 520, 316
 Shakura N.I., Sunyaev R.A., 1973, A&A, 24, 337
 Shimura T., Takahara F., 1995, ApJ, 445, 780
 Skinner G.K., Willmore A.P., Eyles C.J. et al., 1987, Natur, 330, 544
 Skinner G.K., Pan H.C., Maisack M. et al., 1991, A&A, 252, 172
 Sidoli, L., Mereghetti S., 2002, A&A, 388, 293
 Smith D.M., Heindl W.A., Swank J.H., 2002, ApJ., 578, 129
 Strohmayer T.E., 2001, ApJ, 552, 49
 Sunyaev R.A., Churazov E., Gilfanov M. et al., 1991, A&A, 247, 29
 Takahashi T., 2007, PASJ, 59, 35
 Tingay S.J., Jauncey D.L., Preston R.A. et al., 1995, Nature, 374, 141
 Titarchuk L., 1994, ApJ, 434, 313
 Titarchuk L., Mastichiadis A., Kylafis N.D., 1997, ApJ, 487, 834
 Tomsick J.A., Kaaret P., Kroeger R.A., Remillard R.A., 1999, ApJ, 512, 892
 Tomsick J.A., Kalemci E., Kaaret P., Markoff S., Corbel S., Migliari S., Fender R., Bailyn C.D., Buxton M.M., 2008 ApJ, 680, 593
 Ueda Y., Yamaoka K., Remillard R., 2009, ApJ, 695, 888
 Wilkinson T., Uttley P., 2009, MNRAS, 397, 666
 Yamauchi S., Ebisawa K., Tanaka Y. et al., 2009, PASJ, 61S, 225
 Zdziarski A.A., Grove E.J., Poutanen J., Rao A.R., Vadawale S.V., 2001, ApJ, 554, 45
 Zhang S.N., Wilson C.A., Hamson B.A., Fishman G.J., Wilson R.B., Paciesas W.S., Scott M., Rubin B.C., 1994, IAUC 6046
 Zimmerman E.R., Narayan R., McClintock J.E., Miller J.M., 2005, ApJ, 618, 832